



Supporting Online Material for

Aversive Learning Enhances Perceptual and Cortical Discrimination of Indiscriminable Odor Cues

Wen Li,* James D. Howard, Todd B. Parrish, Jay A. Gottfried

*To whom correspondence should be addressed. E-mail: wenli@northwestern.edu

Published 28 March 2008, *Science* **319**, 1842 (2008)
DOI: 10.1126/science.1152837

This PDF file includes:

Materials and Methods

SOM Text

Figs. S1 to S3

Tables S1 and S2

References

Supporting Online Material

Materials and methods

Subjects

A total of 14 healthy subjects (mean age, 26 years; range, 22-35 years; 10 women) provided informed consent to take part in the study, which was approved by the Northwestern University Institutional Review Board. Prior to enrollment in the study, subjects were screened to ensure that the odor enantiomers (detailed below) were perceptually indiscriminable. Two female subjects were excluded due to technical problems with the olfactometer, leaving 12 subjects for the remaining analysis.

Stimuli

We selected two pairs of odor enantiomers, mirror-symmetric (chiral) molecules that have previously been shown to be perceptually indistinguishable in humans (*I*): (+)-rose oxide (11.1%) and (–)-rose oxide (8.3%); and S(+)-2-butanol (3.0%) and R(–)-2-butanol (4.4%). These were all diluted in mineral oil and matched for intensity. The odorants were assigned to four conditions: (1) tgCS+ (target CS+, to be paired with shock), (2) chCS+ (chiral counterpart of tgCS+, no shock), (3) CS– (non-conditioned control odorant, no shock), and (4) chCS– (chiral counterpart of CS–, no shock). Odor delivery during scanning was achieved using an MRI-compatible, 10-channel computer-controlled olfactometer (airflow set at 3 L/min), which permits rapid delivery of odor in the absence of tactile, thermal, or auditory confounds (2, 3).

Experimental paradigm

During the imaging study, subjects participated in an olfactory paradigm of classical (Pavlovian) conditioning, in which the tgCS+ odorant was repetitively paired with mild electric shock (the unconditioned stimulus, or US) to the lower leg. This aversive conditioning session was flanked by pre- and post-conditioning fMRI sessions, and olfactory psychophysical testing was conducted at the start and end of the experiment (see following sections).

fMRI scanning

The imaging part of the learning study consisted of three sessions: pre-conditioning, conditioning, and post-conditioning (**Fig. 1**, main text). There was also an independent odor localizer scan at the end of the experiment. During pre-conditioning (16 min), the four odorants or air (included to help minimize olfactory fatigue and to provide a low-level baseline) were each delivered 15 times in pseudo-random order, such that each trial type was presented equal numbers of times in each third of the session, and no trial type occurred more than two times in a row. Trials recurred with a stimulus-onset asynchrony (SOA) of 12 sec. At the onset of each trial, a visual cue (“Sniff now”) prompted subjects to make a 3-sec sniff, during which time an odorant or air was presented, and subjects were asked to make an odor presence/absence judgment by pressing one of two buttons. Stimulus presentation and collection of responses were controlled using Cogent2000 software (Wellcome Dept., London, UK), as implemented in Matlab.

During the conditioning session (7 min), each odorant was presented seven times, in a manner similar to the pre-conditioning session, except that a brief electric shock (the US) co-terminated with each tgCS+ presentation (see next section). Note that each odorant was presented equal numbers of times during conditioning, to ensure that the learning effects could not be merely explained by greater mere exposure to the tgCS+ stimulus (i.e., minimizing the possibility of non-associative perceptual learning) (2).

The post-conditioning session (19 min) was essentially the same as the pre-conditioning session, except that there were 19 trials for each condition, and four of the 19 tgCS+ trials were re-paired with shock to prevent extinction (these trials were excluded from later analysis to avoid US-related stimulus confounds).

In a final session, an independent odor localizer scan was acquired to isolate functional regions of interest. Four novel odorants (butanol, anisole, 2-heptanol, and α -ionone), neutral in valence (4, 5), relatively unfamiliar, and matched for intensity were each presented four times, in addition to 16 air-only trials, pseudorandomly intermixed. Similar to the conditioning sessions, subjects took part in an odor detection task during this scan.

Psychophysical testing

Subjects participated in a “triangular” odor discrimination test (1), which is frequently used in olfactory studies to assess odor differences in perceptual identity (i.e., the quality or character of a smell emanating from an odorous object). On each trial subjects were

presented with three bottles, two containing one odorant, and the third the chiral counterpart, and were asked to identify the bottle that contained the odd odorant, Subjects were explicitly instructed to focus on odor quality in attempting to discriminate the stimuli. Each of the four odorants was assigned as the odd odorant twice, resulting in a total of 8 trials, which were randomly intermixed. These tests were administered both prior to and following the scanning experiment, providing sensitive measures of odor discriminability between each chiral pair of odorants.

We also considered the possibility that subjects might have used perceptual cues related to odor intensity, valence, or familiarity to guide their choices on the triangular test (even though every subject was instructed to avoid using these cues for odor discrimination). Therefore, both before and after the experiment, subjects also provided perceptual ratings of odor intensity, familiarity, and valence for each of the odorants, using Likert scales ranging from 0 to 10, with anchors “undetectable” and “extremely strong” (intensity), “extremely unfamiliar” and “extremely familiar” (familiarity), and (from –10 to 10) “extremely unpleasant” and “extremely pleasant” (valence). These data were analyzed offline in Matlab using nonparametric statistical tests (Wilcoxon Sign-Rank Test).

Electrical stimulation

Electrical stimulation during conditioning consisted of a single square-wave pulse of current generated by a commercially available stimulator. Electric current intensity and pulse duration were calibrated individually prior to scanning (intensity, 0.5 to 5 mA; duration, 160-400 ms), such that each subject found the stimulation highly uncomfortable

but still tolerable. Following previously published protocols (6, 7), the apparatus is electrically grounded to external housing in the control room of the MRI scanner, and the pulse output is optically isolated from subjects. The electrical stimulus is transmitted via a constant current unit to a pair of MRI-compatible bipolar silver/gold electrodes at the subject's right lower leg. These electrodes were each affixed with a 10 k Ω resistor (30 cm from the electrode tip) to prevent the possibility of magnetically induced currents from reaching the subjects. Within the scanner room, the electrode cables were housed within a tinned copper flat braid to provide additional shielding efficiency. Finally, all participants had quick access to an emergency bell inside the scanner, in the event that the shock became too intense (note this issue did not arise during the study).

Respiratory and SCR monitoring

During scanning, subjects were affixed with a pair of breathing belts to monitor respirations on-line (2, 8). The output from these belts was transmitted to a piezo-resistive differential pressure sensor (0-1 psi), and the resulting analog signal was amplified, digitized, and recorded on a PC computer using a data acquisition system and accompanying software. In subsequent analysis, the subject-specific sniff waveforms were baseline-adjusted by subtracting the mean activity in the 500 ms preceding sniff onset, and then averaged across each condition. Sniff inspiratory volume, peak amplitude, and latency to peak were computed for each condition and entered into repeated-measures ANOVAs for statistical analysis in Matlab. There were no significant differences among odor conditions or between pre- and post-conditioning sessions for

any of these parameters (all p 's > 0.05), ruling out potential confounds related to variations in sniffing.

SCR responses were continuously acquired from two Ag-AgCl electrodes placed on the first and second toes of the subject's left foot, using the PowerLab device and an accompanying SCR pre-amplifier module. These recording electrodes are MRI-compatible and have been modified by inserting an electronic resistor near the subject end, in case of the unlikely scenario that the MRI might induce current flow through the electrode. SCR traces in three out of 12 subjects could not be analyzed due to technical problems. Offline data analysis of SCR waveforms was conducted in Matlab, after low-pass filtering (0.5 Hz) to eliminate MRI scanning artifacts. Evoked SCR responses were characterized by the maximum of the SCR deflection in the interval between 1 and 7 s after stimulus onset. In accordance with prior methods (9), only trials with a minimal evoked deflection of 0.01 μ S were included in the SCR analysis.

Image acquisition

Gradient-echo T2-weighted echoplanar images (EPI) were acquired with blood-oxygen-level-dependent (BOLD) contrast on a 3T MRI scanner, using an eight-channel head coil and an integrated parallel acquisition technique known as GRAPPA (GeneRalized Autocalibrating Partially Parallel Acquisition) to improve signal recovery in medial temporal and basal frontal regions (3). Imaging parameters were: TR, 1.51 s; TE, 20 ms; slice thickness, 2 mm; gap, 1 mm; in-plane resolution, 1.72 x 1.72 mm; field of view, 220 x 206 mm, matrix size, 128 mm. Image acquisition was tilted at 30° to further reduce

susceptibility artifact in olfactory areas. A total of 1,700 volumes (24 interleaved slices per volume covering piriform and orbitofrontal cortices) was obtained over the three experiment sessions, and 270 volumes were acquired for the localizer session. A high-resolution (1 x 1 x 1 mm) T1-weighted anatomical scan was also acquired after functional scanning, and a whole-brain EPI image was obtained to aid with spatial coregistration between the functional (partial) EPI and anatomical images (see below).

fMRI data processing

The imaging data were analyzed in two ways: a conventional (univariate) analysis using the general linear model in SPM2 (www.fil.ion.ucl.ac.uk/spm), and a multivariate analysis using spatial correlation techniques outside of SPM2.

I. Conventional analysis

The fMRI data were pre-processed using SPM2. After the first 8 “dummy” volumes were discarded to permit T1 relaxation, images were spatially realigned to the first volume of the first session and slice-time adjusted. This was followed by spatial normalization to a standard EPI template, resulting in a functional voxel size of 2 x 2 x 2 mm, and smoothing with a 6-mm (full-width half-maximum) Gaussian kernel, aiding multi-subject comparisons.

The pre-processed event-related fMRI data were then analyzed using the general linear model in SPM2. For the *pre-conditioning session*, five vectors of onset times were created, corresponding to the four odor conditions and the air condition. These vectors

were encoded as stick (delta) functions, and then convolved with a canonical hemodynamic response function (HRF) to assemble five event-related regressors of interest for inclusion in the model. Condition-specific temporal and dispersion derivatives of the HRF were also included to account for temporal and spatial variations in the BOLD response. For the *conditioning session*, in addition to the five onset vectors, condition-by-time interactions were modeled using a parametric regressor to estimate response plasticity, by multiplying the onset vectors with an exponential function decaying at a rate of $\frac{1}{4}$ session length (10, 11). For the *post-conditioning session*, modeling was identical to pre-conditioning, except for the inclusion of an additional regressor containing the four tgCS+ events paired with shock, to prevent contamination of the (unpaired) tgCS+ response by the US.

For the *odor localizer session*, only two conditions of interest were specified in the model: an “odor” regressor comprising all trials collapsed across the four odor stimuli, and a “no odor” regressor comprising the air-only trials. For all of the above models, six movement-related vectors (derived from spatial realignment) were incorporated as regressors of no interest, and the data were high-pass filtered (cut-off, 128 s). In a first step, voxel-wise condition-specific beta values (parameter estimates) were estimated for each subject individually, and then in a second step (random-effects analysis), subject-wise comparisons of these parameter estimates, corresponding to particular contrasts of interest, were computed using a series of one-sample t-tests or ANOVAs. Activations were reported in a limited set of brain areas where we had *a priori* regional hypotheses, including anterior and posterior piriform cortex, orbitofrontal cortex (OFC), and

amygdala (2-3, 10-13). Significance threshold was set at $p < 0.001$, uncorrected. All reported voxels correspond to MNI (Montreal Neurological Institute) coordinate space.

Two contrasts were tested. (1) Learning during the acquisition of aversive conditioning. Because amygdala has been shown to habituate rapidly during conditioning (10, 12), we performed a condition-by-time interaction by modeling the conditioning session events with a time-dependent parametric regressor (an exponential decay function with 1/4 session length), in order to examine learning-related response decline in this brain region. We compared [tgCS+ x time] vs. [CS- x time], as well as [chCS+ x time] vs. [CS- x time] to assess generalization of learning to the closely related chiral stimulus. To perform small-volume correction (SVC) of amygdala, we constructed anatomical masks of the amygdala using MRIcro software (15), with reference to the mean subject T1-weighted scan and a human brain atlas (16), following prior methods (2). It is important to note that since the tgCS+ odorant was paired 100% with shock during this phase, we were unable to test main effects of tgCS+ vs. CS- during conditioning, which would have been confounded by the presence of the US. Nevertheless, this was not a problem with the condition-by-time comparisons, since in this type of analysis the shock represented a constant (unchanging) variable that should not have altered the time-course of tgCS+ response decay.

(2) Pre- vs post-conditioning. Here we contrasted response changes in the CS+ stimuli from before to after aversive conditioning, by testing [tgCS+_{post} - tgCS+_{pre}] vs. $\frac{1}{2} * [(CS-_{post} + chCS-_{post}) - (CS-_{pre} + chCS-_{pre})]$, to determine whether odor-shock pairing would

subsequently update neural coding of the tgCS+ odorant. A similar contrast between chCS+ and the CS- pair was conducted to test generalization of this effect to the perceptually related stimulus.

II. Multivariate analysis

Multivariate fMRI analysis offers certain advantages over conventional univariate techniques, helping to preserve spatial-based information at the level of individual voxels, even when there may be no significant differences in mean activation across a particular region of interest (see **Supporting Fig. S1**). This analysis proceeded in several steps. First, we identified odor-active cortex from the independent odor localizer session, on a subject-by-subject basis, by contrasting odor vs no-odor conditions (using model estimation in SPM2, based on normalized, smoothed data), liberally thresholded at $p < 0.5$ uncorrected. These functional regions of interest (ROIs) (*14*) provided a way to constrain anatomical ROIs of piriform cortex and OFC that had been drawn in MRICro (*15*), with reference to a human brain atlas (*16*), and served as a guide for the subsequent voxel selection (discussed below).

Second, all of the fMRI data from the aversive conditioning study were spatially realigned to the first image of the first session and co-registered to the whole-brain EPI scan, while the high-resolution T1-weighted scan was also co-registered to the whole-brain scan, to ensure the data were in spatial register. Note that in all subsequent steps these fMRI data were neither normalized nor smoothed, to preserve signal information at the level of individual voxels, scans, and subjects.

Third, we extracted the fMRI time-series data from each condition and each session during the aversive conditioning experiment, for each voxel contained within the functional ROIs of piriform cortex and OFC. From these we assembled linear vectors of fMRI spatial activity in piriform cortex or OFC, defined for each condition-specific voxel time-series as the peak fMRI signal within a 5-TR interval between 1.5 s and 9 s after odor onset (time window based on the canonical HRF typically peaking at 4-6 s post-stimulus [17, 18]), after baseline correction, by subtracting the minimal fMRI activity in the interval between two TRs (3 s) pre-stimulus and one TR preceding the peak signal. This resulted in a total of 15 pattern vectors for each condition at pre-conditioning, and 15 vectors for tgCS+ (unpaired with shock) and 19 vectors for the other three conditions at post-conditioning. The length of each vector corresponded to the number of activated voxels selected for each subject based on the localizer task (**Supporting Fig. S2**). The voxel order within these linear vectors was arranged in descending order of voxel activity, as indexed by the voxel-specific T-values from the localizer scan.

Finally, condition-specific pattern vectors were averaged across all trials to form mean pattern vectors for both pre- and post-conditioning sessions, which were then used to calculate pairwise spatial correlation coefficients within and between enantiomer pairs (19). Spatial correlation coefficients (R values) were computed between the linear vectors of voxel activity for CS+ pairs (tgCS+:chCS+) and CS- pairs (CS-:chCS-) at both pre- and post-conditioning, following methods described by Haxby and colleagues in visual association cortex (19). Statistical analyses of the spatial fMRI correlations, as

well as the olfactory psychophysical data, were based on non-parametric tests (Friedman test for related samples, and post-hoc Wilcoxon Sign-Rank tests). Significance was set at $p < 0.05$, two-tailed.

Given the well-documented anatomical heterogeneity in the human olfactory system, sometime ranging as high as 8-10 fold even within young age-matched individuals (20-23), we made no group-wise assumptions about how many voxels to include in the spatial correlation analysis. Instead, the number of voxels within each functional ROI was independently determined for each subject, corresponding to the number of voxels at which the spatial patterns of BOLD intensity contained the strongest discriminant validity pre-conditioning, i.e., the greatest correlation difference between *within*-pair odorants and *across*-pair odorants (collapsed across both CS+ and CS- pairs). As a follow-up analysis we examined the level of spatial divergence for across-pair patterns, compared to within-pair patterns, given that the two enantiomers classes (i.e., CS+ pairs and CS- pairs) have distinct structural and perceptual profiles. This showed that at the group level, the *within-enantiomer* correlation (collapsed across tgCS+:chCS+ and CS-:chCS-) was considerably higher than the *across-enantiomer* correlation (collapsed across tgCS+:CS-, tgCS+:chCS-, chCS+:CS-, and chCS+:chCS-) ($p < 0.005$; Wilcoxon test, two-tailed). In addition, the value f , a statistic reflecting the effect size of differences between paired samples (corresponding to Cohen's d), amounted to 0.66, indicating that the correlation difference between within- versus across-enantiomer pairs constituted a large effect by convention (24). Therefore, on the basis of these findings we suggest that the multivariate

technique used here has satisfactory discriminant validity for distinguishing between different odor classes..

Finally, it is important to note that the post-conditioning data were not used in this procedure, to prevent introducing voxel-selection biases into the learning-related effects. In this manner we were able to test whether this odor quality-sensitive voxel ensemble (from *pre*-conditioning) underwent systematic pattern changes as a result of aversive learning (at *post*-conditioning). Nonetheless, when we limited the analysis to the 50 most active voxels in posterior piriform cortex for each subject (**Supporting Fig. S3**), irrespective of pre-conditioning discriminability, we still observed a comparable and significant reduction in the spatial correlation for CS+ (vs. CS-) pairs from pre- to post-conditioning ($p < 0.05$, Wilcoxon test, one-tailed), corroborating our primary approach.

Supporting Text

This section considers four issues of data interpretation in greater detail.

1. Intensity changes as a potential explanation for the odor discrimination effects

We considered the possibility that changes in odor intensity might play a role in the perceptual and neural improvement of odor discrimination, especially since it is known that odor exposure can induce changes in perceived intensity (25). By administering the same number of trials for all four odor conditions throughout the experiment (including during the conditioning phase), we ensured that subjects were exposed equally to all four odorants, such that there might be a general shift in intensity to the odors, but no specific

change to any one odor (in particular the conditioned tgCS+ stimulus). Moreover, the lack of change in mean response magnitude in posterior piriform cortex (which might be expected if there was an intensity difference), along with the lack of changes in anterior piriform cortex (which might be expected if there was an increase in arousal/intensity), would argue against the notion of any substantive influence of odor intensity. Finally, as discussed above, subjects' intensity ratings, collected pre- and post-conditioning, indicated no significant changes due to conditioning or odor type. We thus conclude that intensity effects are unlikely to play a prominent role in this study, although because these null findings cannot be treated as definitive evidence, additional psychophysical measures could be useful for further ruling out intensity differences between conditions.

2. Correlation changes in the posterior piriform patterns of the control (CS-) pair

Inspection of Figure 2B (main text) shows that there was a modest change in the spatial correlation in posterior piriform cortex for the CS- pair (opposite in direction to the CS+ pair), though we note that the absolute change for CS+ was in fact ~70% larger than for CS-. It is worth emphasizing here that the learning effects on the CS+ pair should be interpreted in the context of the CS- pair. Specifically, we reasoned that because of the long duration of the experiment, a control pair of odorants (CS- and chCS-) was necessary in order to gauge olfactory fatigue, habituation, and other time-dependent effects that might have reduced perceptual sensitivity. In this way, we were able to demonstrate that the CS+ pair exhibited a correlation *decrease* (less similar), over and beyond the general trend of correlation *increase* (more similar) as indexed by the control CS- pair.

3. Motivational factors in perceptual plasticity

Motivational or emotional factors, induced by aversive conditioning and arguably guided by the amygdala, could in theory help promote perceptual plasticity in olfactory sensory cortex. Although difficult to explore this possibility directly, we performed two supplementary analyses. First, we performed a linear regression analysis between subject-specific correlation changes in posterior piriform cortex and the magnitude of amygdala activity decay estimated during the conditioning phase, but found no significant relationship ($p > 0.05$ uncorrected). Second, in a similar way, we examined whether the piriform correlation change correlated with the magnitude of amygdala activity from pre- to post-conditioning, but again found only a weak association ($p = 0.02$ uncorrected) between these effects. Therefore, although it is plausible that motivational mechanisms may influence odor coding (presumably indirectly), in the absence of clear supportive data we felt it was more prudent to limit our conclusions to the posterior piriform cortex.

4. Links between piriform and perceptual discrimination

We performed two supplementary analyses to investigate the links between piriform and perceptual changes in odor discrimination on a subject-by-subject basis. The first of these was a correlation analysis. However, because ten of the twelve subjects showed increased odor discrimination (by similar magnitudes) of the CS+ stimuli from pre- to post-conditioning, the distribution of perceptual learning scores was highly skewed and narrow, rendering a small variance (see error bars in Fig. 2A). As a result of attenuation by the limited variance (violating one of the basic assumptions for correlational analysis—*unrestricted variance*), the correlation between piriform discrimination and perceptual discrimination for the CS+ pair was modest,

although still in the predicted direction ($r = 0.19$). In the second analysis, we performed a median-split of the sample into low-learning and high-learning groups (based on their perceptual discrimination scores), and found that the average piriform correlation change (from pre- to post-conditioning) for the CS+ pair was 0.02 for the “low” group versus 0.10 for the “high” group. These data thus implicate corresponding changes in behavior and neural activity following conditioning. Taken together with our central findings, we maintain that the concomitant demonstration of neural and perceptual plasticity (both changing in parallel), within the same group of subjects, provides compelling evidence for a close link between piriform discrimination and odor discrimination.

Table S1. Conditioning-Induced Neural Changes to the tgCS+ Odorant

Brain region	Peak MNI coordinates			Z value
	<i>x</i>	<i>y</i>	<i>z</i>	
(tgCS+ x time) - (CS- x time): time-dependent decreases				
Amygdala				
Right posterior	32	-12	-14	4.41
	28	-8	-18	3.19†
	16	-8	-24	3.15†
Left posterior	-32	-14	-26	3.85
Right anterior	30	-2	-20	3.34*
Left anterior	-32	-2	-32	3.19*
(tgCS+ - CS-)post - pre				
Orbitofrontal cortex				
Right posterior	26	18	-24	3.12
	36	32	-20	3.09
Left posterior	-14	24	-24	3.23

All p 's < 0.001 uncorrected; *, $p \leq 0.05$, corrected for small volume; †, $p < 0.1$, corrected for small volume.

Table S2. Conditioning-Induced Neural Changes to the chCS+ Odorant

Brain region	Peak MNI coordinates			Z value
	<i>x</i>	<i>y</i>	<i>z</i>	
(chCS+ x time) - (CS- x time): time-dependent decreases				
Amygdala				
Right anterior	26	-4	-22	2.94
(chCS+ - CS-)post - pre				
Orbitofrontal cortex				
Right posterior	22	20	-24	3.01
Left posterior	-12	24	-24	2.56

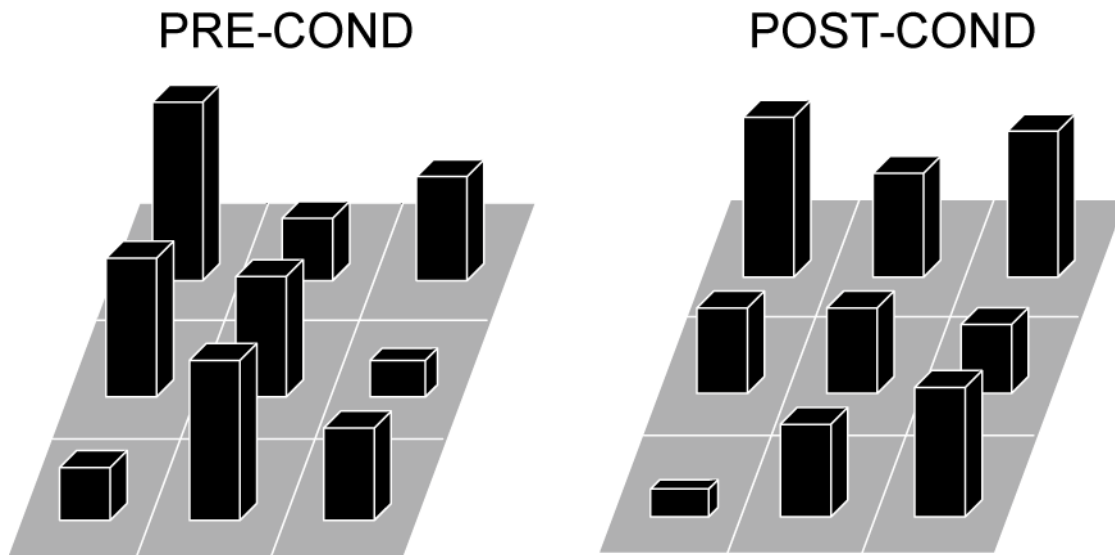


Figure S1. Hypothetical topographical change in fMRI ensemble activity across voxels, in the absence of significant voxel-specific signal change in fMRI activity. This nine-voxel cartoon indicates how olfactory learning could modulate a spatially distributed pattern of fMRI signal intensities across the whole set of voxels, without inducing statistically evident changes in fMRI response amplitude at the level of individual voxels. Note also that any given voxel might exhibit a response activation (signal increase) or deactivation (signal decrease) from pre- to post-conditioning.

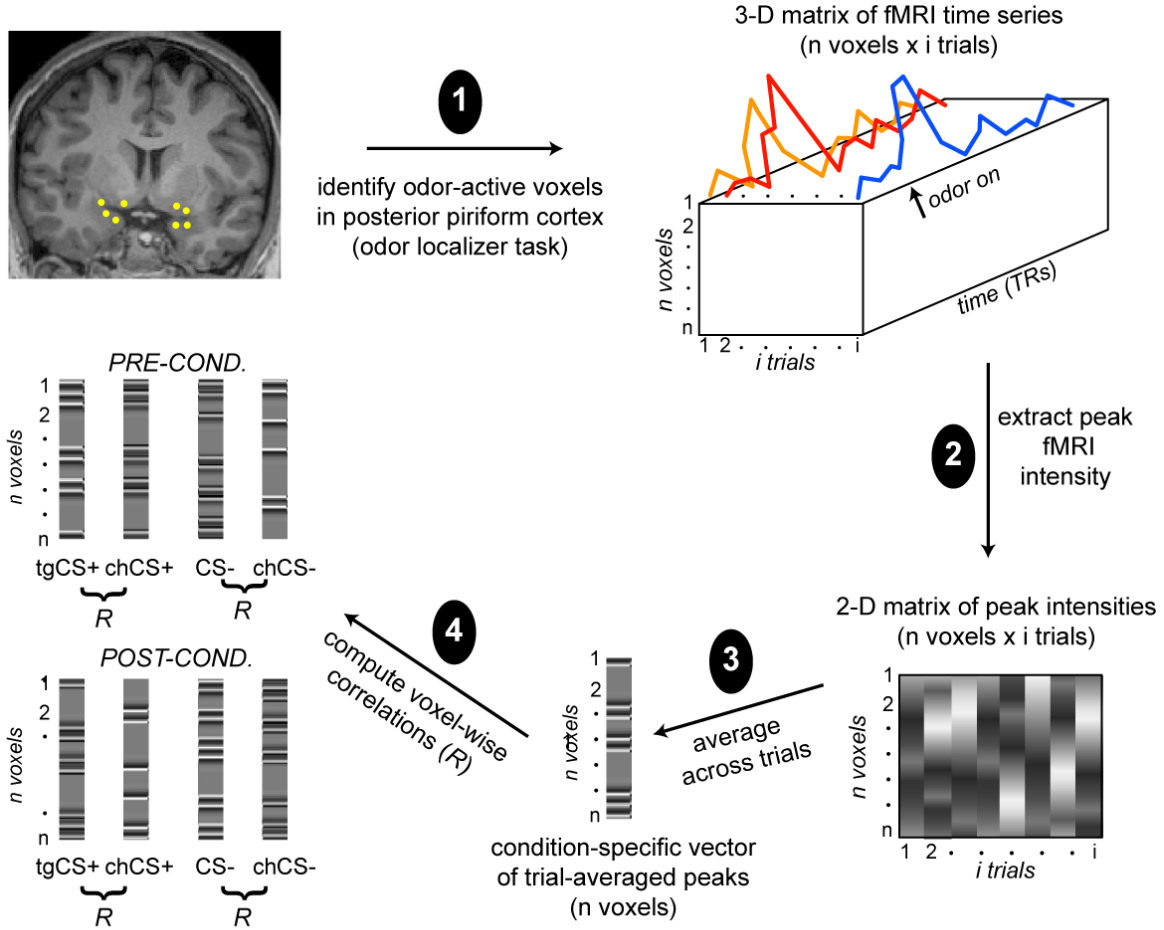


Figure S2. Schematic illustrating the principal methodological steps involved in multivariate analysis of the olfactory fMRI data-set, from selecting voxels (odor localizer task; Step 1) to computing voxelwise spatial correlations (Step 4). Note, the numbers of these steps do not directly match those used in the “Multivariate analysis” section of the Materials and Methods text.

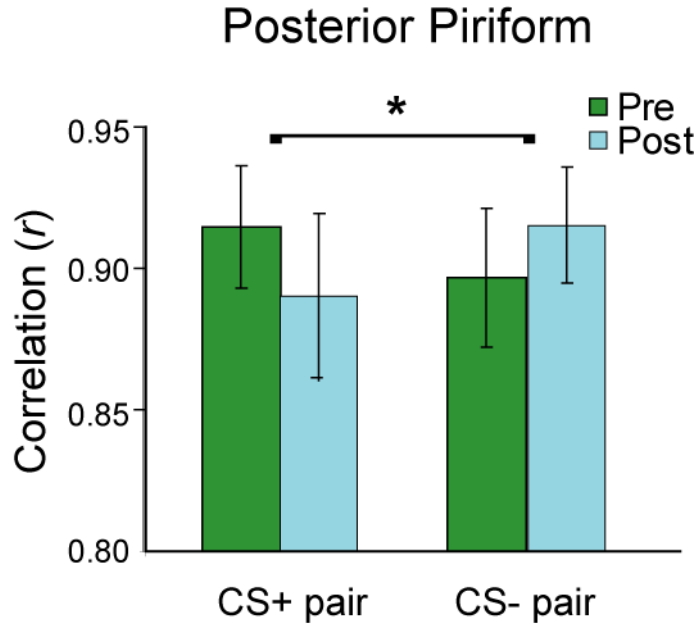


Figure S3. Spatial discrimination for the CS+ pair based on fMRI intensity in the 50 most active posterior piriform voxels from each subject. The learning-induced spatial divergence in piriform activity patterns for the CS+ odorant pair (decreased correlation) significantly differed from the patterns for the CS– pair ($p < 0.05$; Wilcoxon test, one-tailed) and was comparable to results reported in the main text (Fig. 2B) based on individually determined optimal voxel numbers.

Supporting References

1. M. Laska, P. Teubner, *Chem. Senses* **24**, 161 (1999).
2. W. Li, E. Luxenberg, T. Parrish, J. A. Gottfried, *Neuron* **52**, 1097 (2006).
3. J. A. Gottfried, J. S. Winston, R. J. Dolan, *Neuron* **49**, 467 (2006).
4. J. A. Gottfried, R. J. Dolan, *Nat. Neurosci.* **7**, 1144 (2004).
5. J. S. Winston, J. A. Gottfried, J. M. Kilner, R. J. Dolan, *J. Neurosci.* **25**, 8903 (2005).
6. A. O. Hamm et al., *Brain* **126**, 267 (2003).
7. C. M. Thiel, *Neurobiol. Learn. Mem.* **80**, 234 (2003).
8. J. A. Gottfried, R. Deichmann, J. S. Winston, R. J. Dolan, *J. Neurosci.* **22**, 10819 (2002).
9. A. Flykt, F. Esteves, A. Ohman, *Biol. Psychol.* **74**, 328 (2007).
10. C. Buchel, J. Morris, R. J. Dolan, K. J. Friston, *Neuron* **20**, 947 (1998).
11. J. A. Gottfried, J. O'Doherty, R. J. Dolan, *J. Neurosci.* **22**, 10829 (2002).
12. K. S. LaBar, J. C. Gatenby, J. C. Gore, J. E. LeDoux, E. A. Phelps, *Neuron* **20**, 937 (1998).
13. E. A. Phelps, *Annu. Rev. Psychol.* **57**, 27 (2006).
14. C. Zelano et al., *Nat. Neurosci.* **8**, 114 (2005).
15. C. Rorden, M. Brett, *Beh. Neurol.* **12**, 191 (2000).
16. J. K. Mai, J. Assheuer, G. Paxinos, *Atlas of the Human Brain* (Thieme, New York, 1997).
17. A. M. Dale, R. L. Buckner, *Hum. Brain Mapp.* **5**, 329 (1997).
18. K. J. Friston et al., *Neuroimage* **7**, 30 (1998).
19. J. V. Haxby et al., *Science* **293**, 2425 (2001).
20. C. G. Smith, *J. Comp Neurol.* **77**, 589 (1942).
21. K. P. Bhatnagar, R. C. Kennedy, G. Baron, R. A. Greenberg, *Anat rec* **218**, 73 (1987).
22. P. M. Goncalves Pereira, R. A. P. Insausti, E., T. Salmenpera, R. Kalviainen, A. Pitkanen, *Am J Neuroradiol.* **26**, 319 (2005).
23. P. Rombaux et al., *Arch Otolaryngol Head Neck Surg* **132**, 1346 (2006).
24. J. Cohen, *Statistical Power Analysis for the Behavioral Sciences* (Hillsdale, NJ, ed. 2nd, 1988).
25. P. Dalton, N. Doolittle, P.A. Breslin, *Nat. Neurosci.* **5**, 199 (2002).